



Article

# Projecting Barrier Beach Vulnerability to Waves and Sea-Level Rise Under Climate Change

Andrea Sulis <sup>1,\*</sup>, Fabrizio Antonioli <sup>2</sup> , Andrea Atzeni <sup>3</sup>, Andrea Carboni <sup>1</sup>, Giacomo Deiana <sup>4,5</sup> , Paolo E. Orrù <sup>4,5</sup>, Valeria Lo Presti <sup>6</sup> and Silvia Serreli <sup>7</sup>

<sup>1</sup> Department of Architecture, Design and Urban Planning, University of Sassari, 07041 Alghero, Italy; a.carboni6@studenti.uniss.it

<sup>2</sup> CNR, IGAG, 00185 Roma, Italy; fabrizioantonioli2@gmail.com

<sup>3</sup> Department of Civil and Environmental Engineering and Architecture, University of Cagliari, 09123 Cagliari, Italy; atzeni.a@libero.it

<sup>4</sup> Department of Chemical and Geological Sciences, University of Cagliari, 09042 Monserrato, Italy; giacomo.deiana@unica.it (G.D.); orrup@unica.it (P.E.O.)

<sup>5</sup> CoNISMa Interuniversity Consortium on Marine Sciences, 00126 Roma, Italy

<sup>6</sup> Department of Mathematics and Computer Sciences, Physical Sciences and Earth Sciences, University of Messina, 98122 Messina, Italy

<sup>7</sup> Department of Humanities and Social Sciences, University of Sassari, 07100 Sassari, Italy; serreli@uniss.it

\* Correspondence: asulis@uniss.it

**Abstract:** Long-term impacts of sea-level changes and trends in storm magnitude and frequency along the Mediterranean coasts are key aspects of effective coastal adaptation strategies. In enclosed basins such as a gulf, this requires a step beyond global and regional analysis toward high-resolution modeling of hazards and vulnerabilities at different time scales. We present the compound future projection of static (relative sea level) and dynamic (wind-wave) impacts on the geomorphological evolution of a vulnerable sandy coastal plan located in south Sardinia (west Mediterranean Sea). Based on local temporal trends in  $H_s$  ( $8 \text{ mm yr}^{-1}$ ) and sea level ( $5.4 \text{ mm yr}^{-1}$ ), a 2-year return time flood scenario at 2100 shows the flattening of the submerged morphologies triggering the process of marine embayment. The research proposes adaptation strategies to be adopted to design the projected new coastal area under vulnerabilities at local and territorial scales.

**Keywords:** sea level rise; wave height trend; barrier beach; vulnerability; La Playa beach



Received: 18 November 2024

Revised: 27 December 2024

Accepted: 2 January 2025

Published: 3 February 2025

**Citation:** Sulis, A.; Antonioli, F.; Atzeni, A.; Carboni, A.; Deiana, G.; Orrù, P.E.; Lo Presti, V.; Serreli, S. Projecting Barrier Beach Vulnerability to Waves and Sea-Level Rise Under Climate Change. *J. Mar. Sci. Eng.* **2025**, *13*, 285. <https://doi.org/10.3390/jmse13020285>

**Copyright:** © 2025 by the authors. Licensee MDPI, Basel, Switzerland. This article is an open access article distributed under the terms and conditions of the Creative Commons Attribution (CC BY) license (<https://creativecommons.org/licenses/by/4.0/>).

## 1. Introduction

Coastal adaptation strategies require a full understanding of local relative sea-level change. Due to increased rates of land-ice melting and ocean thermal expansion [1], the global mean sea level (GMSL) has been dramatically rising in a highly non-uniform pattern. Previous studies [2,3] show how past sea-level changes in the Mediterranean Sea have deviated from GMSL trends and how large-scale circulation changes in the basin have produced internal spatial variation. The average rate of sea-level rise in the Mediterranean Sea increased from  $-0.3 \pm 0.5 \text{ mm yr}^{-1}$  in the period 1960–1989 to  $3.6 \pm 0.3 \text{ mm yr}^{-1}$  in 2000–2018 [4]. The main sources of information on long-term sea-level changes in the Mediterranean Sea are tide gauge records (archive of the Permanent Service for Mean Sea Level, <https://www.psmsl.org/>) with low geographic density and relatively long records along the European coasts and satellite altimetry observation with better spatial coverage but on shorter intervals (Sea Level Climate Change Initiative (CCI) project of the European Space Agency (ESA), <https://climate.esa.int/en/projects/sea-level/>), accessed

on 10 November 2024). Long-term impacts of sea-level changes along the Mediterranean coasts have gained the attention of the international scientific community specifically on the dynamics of coastal erosion, groundwater salinization, and change in natural ecosystems (e.g., [5]).

Interest in changes in local wind-generated wave climate both historically and for future projections is quite recent (see, for instance, [6]). Aside from a few studies [7–9], a reliable analysis of the long-term trends in wind-wave extremes under future climate change scenarios is lacking, and this results in a lack of consensus on whether the frequency or magnitude of these extreme events is affected by climate change. Ref. [7] estimated future projections at the end of the 21st century (2081–2100) in 100-year return period significant wave heights ( $H_{s,100}$ ) under two IPCC representative greenhouse gas emission scenarios (Representative Concentration Pathways (RCPs): RCP4.5, intermediate emissions scenario, and RCP8.5, high-emissions scenario) using an intermodel ensemble of seven global wave model runs (WAVEWATCH III v3.14 wave model) forced with independent GCM surface winds, part of the international Coupled Model Intercomparison Project 5 (CMIP5). They found that the Northern Hemisphere shows an irregular pattern, and only the projected decrease in  $H_{s,100}$  of –5 to –15% in the mid and low latitudes of the North Atlantic basin is statistically significant.

Ref. [8] compared significant wave height climatologies and trends over the recent satellite era (1992–2017) from four recent high-quality global datasets (two products based on satellite altimetry, including products by ESA CCI for Sea State and [10], and two ERA5-based reanalysis and hindcast surface wave products from the European Centre for Medium-Range Weather Forecasts (ECMWFs)). The use of data buoys to study long-term sea state variability from reanalyses and hindcast models is fraught with problems associated with the consistency of buoy output and validation methodologies. Although the long-term consistency and accuracy of multimission satellite data depend on careful calibration and quality control (see, for instance, [10]), these data are attractive in long-term analysis of ocean wave climate, thanks to their global coverage, fine spatial resolution, and regular temporal revisits. Trends were estimated by [8] for all the above products for the period 1992–2017 at each  $2^\circ \times 2^\circ$  grid cell over the full globe using linear regression. While substantial differences in climatologies and trends between the products exist, the trends in seasonal mean  $H_s$ , over most of the globe, lie within  $\pm 1 \text{ cm yr}^{-1}$  for all products. However, the North Atlantic shows much smaller changes, which are generally not statistically significant and with no clear sign (i.e., increasing or decreasing). Finally, trends for the buoy data were estimated using both linear and Theil–Sen models [11,12], with similar results as also reported by [13]. Comparing the Theil–Sen slopes with four different models (seasonal Autoregressive Integrated Moving Average, multiple regression modeling, and Generalized Additive Model modeling), ref. [14] found that the different approaches result in reasonable agreement for detecting long-term trends of  $H_s$  in the North Atlantic.

In enclosed basins such as a gulf, the waves have properties that are rather different from those in a large environment. This is mainly due to their local generation, and they depend more on the quality of winds (coastal orography) and transformation (bathymetry). The signals on the effects of climate change in the Mediterranean are not univocal; in some cases, a reduction in wave energy has been recorded [15] and the local climate intensification of the waves more frequent [16,17] for meteorological events linked to winds from the south. Extratropical cyclones are the dominant feature of mid-latitudes [18] as in the Mediterranean basin. They mainly form and grow via baroclinic instability, with the available potential energy being proportional to the variance in temperature in the troposphere [19]. Events with a typical radius of 500 km and an average duration of 28 h [20] and many subregional and mesoscale effects take place producing a large spatial

and seasonal variability. Once the suitability of the Theil–Sen slope for detecting long-term trends is shown, in a pioneer high-resolution analysis of wave climate trends, ref. [21] evaluated the spatial distribution of long-term trends of the extremes and the mean  $H_s$  in the Mediterranean Sea based on the hourly 40-year hindcast time series (1979–2018) [22]. While some analogy with the results presented by [10], ref. [21] showed significant regional variations, the most significant trends in annual maximum  $H_s$  being between  $5 \text{ cm yr}^{-1}$  and  $3 \text{ cm yr}^{-1}$  with positive trends in east Sardinia. The mean and the 98th percentile of  $H_s$  produced trend intensities of  $\text{mm yr}^{-1}$  and positive trends in west Sardinia. Ref. [23] showed that projected future wave power in the Mediterranean coast of Morocco is very similar to that of the present considering the whole area, although at some specific points, there are slight changes that are more evident for the RCP8.5 scenario. Results show a significant increase in the temporal variability of wave power in future scenarios, in particular for RCP8.5. Projected future regional wave climate scenarios at a high temporal-spatial scale (25 km and 3 h) were performed by [24] with the SWAN wave model [25] for the NW Mediterranean Sea, using five combinations of regional–global circulation models (RCMs) forced by the increasingly used midline A1B scenario [26]. For the mean climate, relative changes in significant wave heights ( $H_s$ ) up to  $\pm 10\%$  were obtained, whereas they were around  $\pm 20\%$  for the extreme climate; also, higher intensity and number of storms coming from E-SE directly affect the wind–sea/swell distribution of coastal stretches that face east, like the Catalan coast.

In micro- and meso-tidal environments, such as those found in the Mediterranean Sea, extreme wave analysis (e.g., [27]), long-term trend detection [10], and under future climate change scenarios [28], all based on high-quality  $H_s$  dataset over many spatial and temporal scales, may have strong implications for urban and spatial coastal planning. All those tools have proved to be effective in defining scenarios for a decision-making process that planners can guide according to future perspectives on urban behaviors [29]. The scenarios in urban plans at the local level should be multidimensional mainly composed of the dimension of climate change to which this article gives large emphasis, the ecological and historical dimension linked to the need for the protection of the natural heritage and historical–archaeological sites, and the settlement and infrastructural dimension that responds to the need to increase a metropolitan system strengthening.

Based on a widely used methodology, the main novelty of this work is the compound future projection of static (sea level) and dynamic (wind-wave) impacts on the geomorphological evolution of a vulnerable sandy coastal plain. Specifically, we analyzed the submersion dynamics of the lagoon barrier systems [30–32] located in the south Sardinia (west Mediterranean Sea) forced by the Sea-Level Rise (SLR) process as a sum of tectonic mobility, glacio-hydro-isostatic component and induced geomorphological and sedimentological processes of the area, and trends in wave parameters. All these forcings make dramatically complex the projection on the impacts of climate change in this marine-littoral (beach system) and transition (lagoons and river mouth) environments. The research group is questioning the possible effects that a construction process of design scenarios can have on the planning of urban transformations of the territory of La Playa. It is being investigated the significant effects of local and territorial vulnerabilities under the climate projections.

## 2. Materials and Methods

### 2.1. Geomorphological Context

The continental margin of Southern Sardinia (Figure 1) is characterized by a submarine depositional system, controlled by Pliocene distensive tectonics. It is divided into several marginal basins with the sedimentary contributions of the various segments of the continental shelf [33]. The structure of the southern Sardinian continental margin, as reported

in numerous seismic profiles acquired from the 1970s, is characterized by the succession of two deformational regimes. The oldest corresponds to a compressive phase of crustal thickening that occurred during the Oligocene–Miocene, contemporary to Sardinia–Corsica microplate rotation and opening of Alghero–Provencal. The most recent is associated with the phase of rifting of the Tyrrhenian Sea, when tectonics led to a slight thinning of the Earth’s crust. Cagliari basin is the innermost part of the sedimentary system of the entire margin, delimited and controlled by tectonic blocks of the southern Sardinian continental margin, in particular by the movements of Mount Ichnusa and Su Banghittu submarine blocks [33,34]. The morphostructural characters control the southern Campidano and affect the appearance of the continental shelf and slope in the Gulf of Cagliari; in fact, it is possible to recognize the continuation of the Campidano Graben in the submerged area.

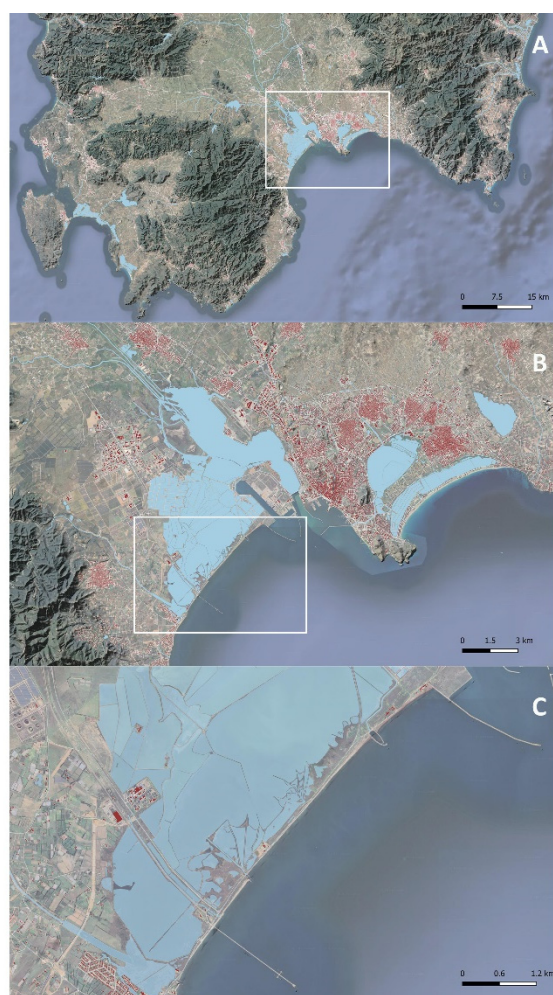


**Figure 1.** Geographic location of the study area: (A) Sud Sardinia Island, Italy; (B) Cagliari Gulf on the South Sardinia; and (C) the coastal strip of La Playa beach between the Santa Gilla Lagoon and the Mediterranean Sea.

The transition to Holocene marine deposits is marked by deep incisions found in both the coastal plain and continental shelf; these paleo-valleys began their evolution after the Last Interglacial highstand, while the highest incision was carved during the MIS 2 lowstand. The Holocene sea-level rise has been detected through studying and dating (14C analyses): Seven orders shelf of beach-rock outcropping on the continental shelf the deepest of lay at  $-45$  m shows ages between 9.5 and 9.9 thousands of years (ky) BP [35,36], while not cemented relict beaches bordered the paleo-lagoon ( $-39$  m) and in the

inner band (−35 m) have recently been identified and sampled the submerged back-shore sand dunes [37].

A buried Punic (2.5 ky BP) paleo-sea level at −2 m is preserved in the bottom-area Santa Gilla lagoon [38–40].

Santa Gilla Lagoon is located on the W-side of Cagliari (39°12′59″ N; 09°02′39″ E). It is a NW–SE orientated depression and roughly deltoid in shape. It connects in the S to the Mediterranean Sea through a narrow channel. On the N shore, the lagoon has two major freshwater inflows from the Flumini Mannu and Cixerri rivers. The average water depth is 1 m, with a maximum of 2 m in the artificial channel connecting the lagoon with the sea.

The lagoon was formed by the fluvial erosion of Quaternary sediment and was successively filled by the sea during the Holocene as a consequence of combined climate fluctuations and subsidence actions. After the sea's Würm regression (stage 2, 15/18 ky), which produced strong erosion of the Tyrrhenian marine sediment ("Panchina Tirreniana" Auct.), the erosional valley was separated from the seawater by a coastal sandy bar that already existed in the Pre-Roman Age. This was filled with, mainly sandy-silt, sediment to a thickness of about 50 m from the upper Pleistocene to the present. The silty sand with subordinate gravel, which is attributed to the alluvial contribution of the Flumini Mannu and Cixerri rivers, creates sedimentary bodies on the NW shore of the lagoon.

The sedimentary succession of the lagoon (Figure 2) starts with fluvial and deltaic sediments (sand, gravel, mud, clay), which is attributed to the end of the MIS6 stage and contains grey-greenish lenses with oysters and peat layers. This sediment is followed by the alternation of littoral fine sand and lagoonal silty sand. Based on the ecology of the coralliferous bioconstructions, it is possible to assume that this reef was located at approximately −5 m during the maximum high-stand phase ( $7 \pm 2$  m). During the building of the modern harbor, a yellowish sandy layer (0.5 m thick) with a *Strombus bubonius* (= *Persististrombus latus*) assemblage attributed to the Last Interglacial cycle (MIS 5.5, 125 ky; [41,42]) was also discovered at a depth of 8 m. A paleo-thalweg is recognizable at a depth of 40 m and testifies to the ancient fluvial incision. Heterometric polygenic gravel from alluvial terraces was sampled between a depth of 30 and 35 m. The infilling of the ancient fluvial valleys is composed of material related to the last phases of the Holocene transgression. This consists of muddy fluvial and deltaic sediments containing more gravel in the lower part and becoming muddy upwards. Beach rocks (−1/−1.5 m depth) have been found in the submerged beach of La Playa, whereas typical rocks of the sabkha environment [35,43] are also present on the edge of Santa Gilla Lagoon [44].

Minor subsidence of 3.5 m in 5 ky, which is mainly attributable to the constipation process of plastic and peat, has been documented both on the continental shelf in the Santa Gilla Lagoon mouth area [36] and along the round lagoon bands, where the high-medieval settlement of Santa Igia (8th–13th century BC; [40]) shows an average lowering of about 1.5 m. GPS measurements evidenced S Sardinia translational movements in a W-SW prevailing direction at speeds of about 1–3 mm yr<sup>−1</sup> [45].

Erosional processes have affected the coastal system over the past decades, with a shoreline retreatment speed of up to 1.5 m yr<sup>−1</sup>.

In the innermost area of Santa Gilla Lagoon, and during particularly intense meteoric events that correspond with extreme rainfall occasions (return time of 5 years), the lagoon hydraulic level significantly increases (about +1.5 m above sea level), causing the flooding of agricultural plains and surrounding urban areas [46].

The comparison between the geochronological data deriving from drills [36] and the projections of the isostatic model [47] allows us to confirm that the E coastal plain of Cagliari, and consequently Santa Gilla Lagoon, is an area characterized by low tectonic activity and subsidence processes (about −0.5 mm yr<sup>−1</sup>). The infilling deposit (peat and

muddy sands) of the axial zone of the river paleo-valley may reach a thickness of about 40 m. Compared data retrieved in two other analog sites: “Portus Herculis” at Malfatano [48] and the submerged building at Sant’Antioco Lagoon [41] confirm the reliability of glacial-hydro isostatic adjustment (GIA) modeling prediction models reconstructed for the entire basin of the Mediterranean Sea [47].

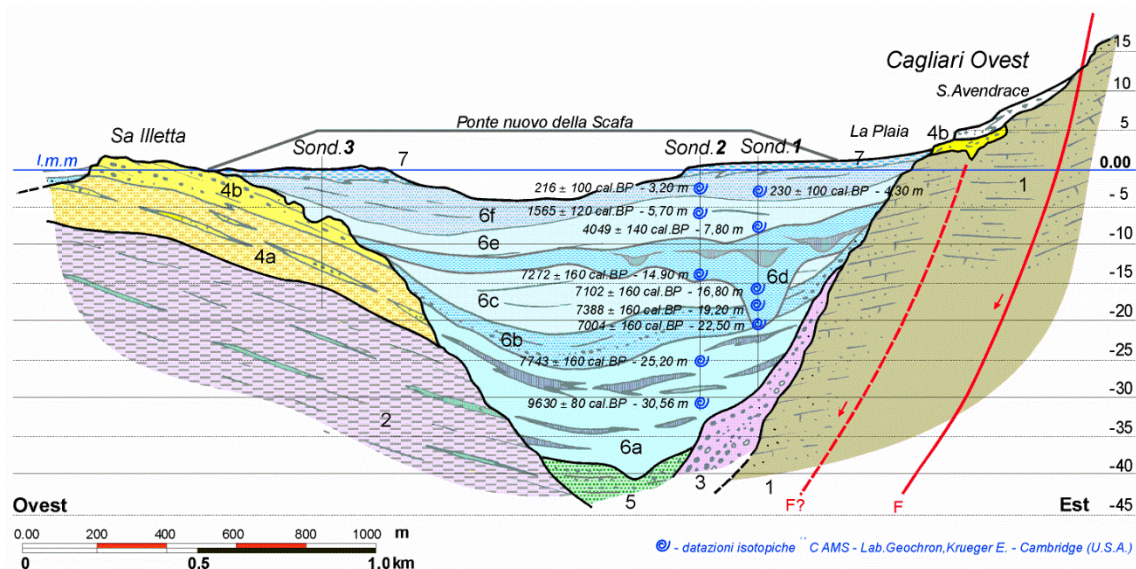


**Figure 2.** Geological section at the mouth of the Santa Gilla lagoon; three stratigraphic surveys provide a breakdown of filled Holocene [36] of the deep valley of the River Mannu paleo-Cixerri (MIS 2—Upper Pleistocene) during the Holocene eustatic rise. Legend: (1) sandstone and marl sandstones (Miocene); (2) deltaic complex in silt and sandy silt with clay and sand with *Ostrea* sp. in lenses (Middle Pleistocene); (3) polygenic gravels in clay matrix (middle Pleistocene); (4a) weakly cemented sands and silty sands yellowish to bioturbation and *Strombus bubonius* (= *Persististrombus latus*) (MIS 5—Upper Pleistocene); (4b) sandstones and microconglomerate with *Cladocora coespitosa*—149 ± 10 kyr BP [41] (MIS 5e—Upper Pleistocene); (5) polygenic gravel with sandy matrix (MIS 2—Upper Pleistocene); (6a) deltaic silt and sandy silt paralic (Yunger Dryas); (6b) littoral sandy silt and silty sands with interbedded peat in *Posidonia oceanica*; (6c) alternating littoral fine sands and silty sand lagoon; (6d) succession of erosional surfaces and filled with sandy silt and sand bioclastic lagoon; (6e) for marine–coastal sands with interbedded thin peaty *Posidonia oceanica*; (6f) lagoonal organic sands and silts; (7) silt and organic and anthropogenic deposits.

### 2.2. SLR Analysis

The global sea-level rise rate SLR in recent decades is around 2 mm yr<sup>-1</sup> (IPCC AR6), but locally vertical ground movements, either due to tectonic activity (subsidence or uplift) [49,50] or sedimentary subsidence, significantly modified the relative submersion rates of coastal plains. Numerous studies have presented forward-looking hypotheses on the global sea-level rise for 2050 and 2100 [51,52] including Sardinia coastal areas. Sea-level change along the Italian coast is the sum of eustatic, Glacial Isostatic Adjustment (GIA), and tectonic factors. The first is global and time-dependent, while the latter two also vary with location. The glacio-hydro-isostatic part exhibits a well-defined pattern and is readily predictable, whereas the tectonic component exhibits a less regular pattern that is generally of shorter wavelength and also less predictable. Together, these components result in a complex spatial and temporal pattern of relative sea-level change around the central. For the eustatic portion, we use IPCC AR6, and for GIA, the Lambek Model, as regards tectonic, we consider this portion of Sardinia stable, with few subsidence in the coastal area of La Playa. In any case, the sum of the 3 vertical movements is given by the tide gauges. The data of sea-level rise projections for Santa Gilla lagoon were recently analyzed, and geological–stratigraphic, geomorphological, and geophysical data used in combination were analyzed

by comparing them with high-dimensional three-dimensional terrain models [31,53]. This interpretative model was subsequently extended and validated in numerous other cases both in the Italian peninsula and in other coastal plains of the Mediterranean [31,32]. The methodology was further investigated by comparing the forecast hypotheses of the drowning of the coastal plains with the data of the Last Interglacial, data that can be obtained from the field investigations on the tidal notch or on the depositional sequences of MIS 5.5, producing a sea-level rise of  $1.3 \text{ mm yr}^{-1}$  in relation to a significant impact of evaporation processes. Another factor that intervenes at the local level in the Santa Gilla lagoon is the glacial and hydroisostatic adjustment (GIA) [54]. Paleolevel indicators (surveys, beachrocks, submerged archaeological structures) in the study area have allowed us to verify the geophysical models of the GIA [47,55]. The GIA component in the western Mediterranean is controlled both by the water load and by the readjustment of the mantle causing a current uplift of the sea in Sardinia of  $0.7 \text{ mm yr}^{-1}$ .

The complexity of geochronological data collected on the sea-level rise starting from about 20 ky cal BP using the various paleo-marine level indicators (e.g., tidal notches, paleo-cliffs, depositional terraces, beachrocks, and fossiliferous deposits) in Santa Gilla lagoon has made it possible to reconstruct the SLR curves comparing them with the predicted curves indicating a general trend towards a Next Interglacial Highstand [54] also in relation to orbital variations [56,57] with values up to  $3.2 \text{ mm yr}^{-1}$  in the last 2 decades at a global level (IPCC RCP 8.5). The last scenario added to the IPCC AR6 report for the Mediterranean regional area highlights the data of Cagliari, which is  $0.78 \pm 0.3 \text{ m}$  at 2100.

### 2.3. Wave Dataset

Long-term changes in sea states are relevant to climate research and coastal applications in Sardinia. The use of data buoys for long-term detection is affected by long-term temporal coverage and consistency of data output (e.g., [58]). Also, the high costs of this direct wave measurement make the spatial coverage and resolution unfit for many engineering applications. The buoy located in the Gulf of Cagliari is part of the Italian Data Buoy Network (RON). RON in Cagliari started in 2002 (Figure 3) but the change in sensors in 2009 and prolonged data losses due to malfunction limit significantly its use.

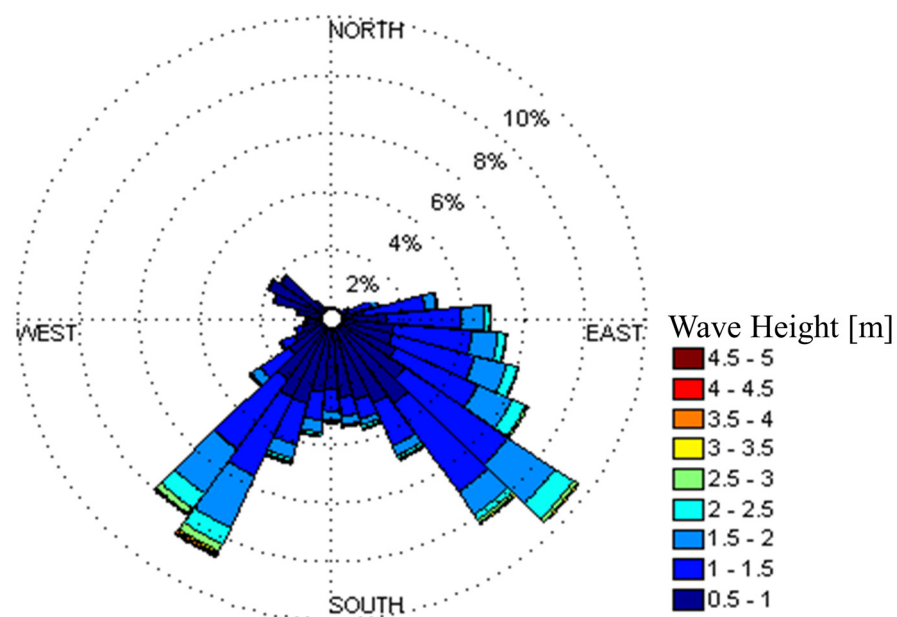


**Figure 3.** RON buoy location in 2014. ID Cagliari buoy is 61221 ( $39^{\circ}06'54'' \text{ N}$ ;  $09^{\circ}24'18'' \text{ E}$ ; 150 m depth).

Multimission satellite data in Sardinia are very attractive for their fine spatial resolution and regular temporal revisits (Ribal and Young, 2019) [10]. Some hindrances still come from the long-term consistency and accuracy of these data [59]. The ESA-CCI is a program of the European Space Agency, whose objective is to realize the full potential of global Earth Observation archives established by ESA and its member states. The Sea State CCI dataset v1 is freely available on the ESA CCI 10 website (<http://cci.esa.int/data>, accessed on 10 November 2024) with three available products: a multimission along-track L2P product, a daily merged multimission along-track L3 product and a multimission monthly gridded L4 product [60,61]. The Sea State CCI dataset in this study is made of altimeter data used from multiple missions spanning from 1996 to 2020. ESA-CCI has been recently intercompared using a consistent methodology (Timmermans et al., 2020) [8] to analyze temporal trends in annual mean significant wave height ( $H_s$ ) over 1992–2018 from a  $2^\circ \times 2^\circ$  grid in the west Mediterranean Sea.

In our analysis at the regional scale of wind-wave trends, we used the assumption already presented by [13]. From the multimission-gridded ( $1^\circ$ ) ESA CCI Sea State dataset, the closest deep-water data point to the Sardinia shoreline was assigned as representative of shoreline conditions. The assumption is that the pattern along the coast of deep-water trends will be representative of nearshore trends. Through a numerical model, future projections in 2050 and 2010 of deep-water extreme significant wave heights at specified return time ( $H_{s,TR}$ ) were transferred to nearshore areas. Details of the adopted numerical model are presented by [29]. Seasonal properties of wave climate in the Western Mediterranean Sea clearly reflect the wave energy distribution in the Northern Hemisphere.

#### 2.4. Settlement and Territorial Context

S.Gilla lagoon, as closed by the coastal barrier beach of La Playa, is a receptor basin for an extensive hydrographic system (Rio Flumini Mannu and Rio Cixerri) (Figure 4). The settlement system still suffers from the hierarchical urban model, with a strong dependence on the capital Cagliari (in terms of mobility for work, services, and leisure activities). This makes the road infrastructure SS195 in La Playa area (Figure 4), a strategic space connecting different settlements. In the coastal area of Capoterra, small residential and tourist villages are growing, involving a wide range of new accommodation activities producing high flows of interference with those generated by the industrial areas.

Two opposing urban dynamics can be recognized in the lagoon territorial context: one concerning the historical–ecological dimension and the related environmental protection, and the other one related to the complex urban processes and infrastructural modifications.

The lagoon is an ecosystem of exceptional natural–historical value. It covers an area of 15,000 hectares, and despite artificial transformations, the natural system has adapted, creating natural habitats for several resident and migratory bird species. This is a Special Protection Area (ZTS in Figure 4) according to the European Union’s “Birds Directive”, which preserves and restores biodiversity. In addition, it is a lagoon of international rank under the Ramsar Convention. It also falls within the Site of Community Interest (SIC in Figure 4) “Stagno di Cagliari, Saline di Macchiareddu, Laguna di Santa Gilla” (ITB040023), belonging to the Natura 2000 Network.

From a historical point of view, the lagoon has many historical and archaeological sites and various land and underwater archaeological heritages (historical harbors, for example). Human settlements in the lagoon date back to the Nuragic period (c. 17th–7th B.C.). Research on settlements from the Phoenician and Punic periods (8th century B.C. and 3rd century B.C.) highlights harbor structures and activities on the eastern coast of the lagoon itself. Due to the facility with which boats could approach the coast, and the natural predisposition of that coastal zone to host port infrastructures [62], the lagoon was an



attraction for human settlements. In addition to the suburb that dates back to the period of the Punic–Roman Carales, on the eastern shores of the lagoon and in the north-western sector of Cagliari, studies and historical–archaeological research point to the villa of Santa Ygia (or Gilla, or Ilia, or Gilia) of the Middle Ages. In the first half of the 13th century, it was the main urban center of the Giudicato of Cagliari [62]. A church, dedicated to St Peter, survives from this villa, between the road and the railway infrastructure in the lagoon border. The lagoon and river sediments, and sediments of marine ingressions, have covered important ancient port structures. These were discovered by the reclamation, drainage, and filling works of the 20th century.

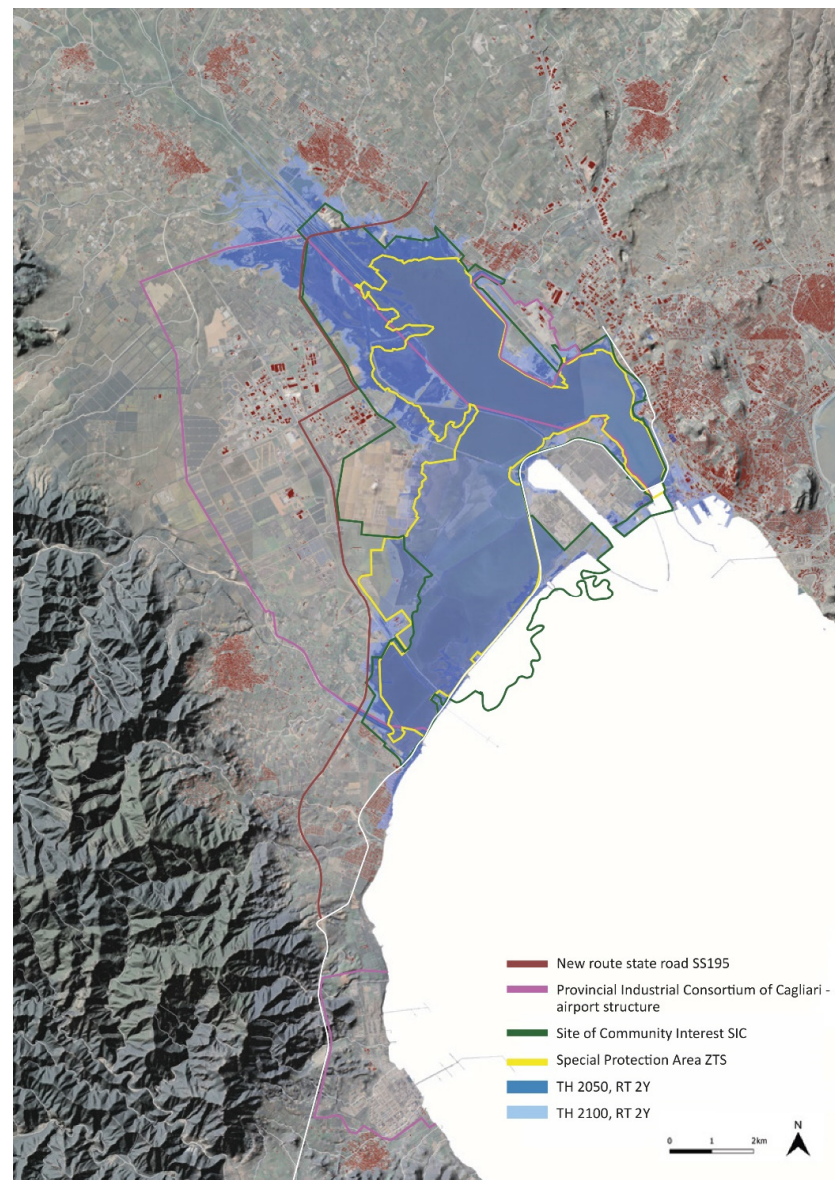


**Figure 4.** The territorial and urban context of the Santa Gilla lagoon in the Cagliari Gulf.

Currently, the study area includes regional-level transport infrastructures, namely, the commercial and industrial Canal Port, the shipbuilding hub, the regional airport, the railway line, and the regional-level road network. The state road SS195 is a strategic connection between these different elements of the lagoon area. The Cagliari Provincial Industrial Consortium includes the industrial areas of Elmas, Sarroch, and Machiareddu. The latter, in an area of approximately 8200 hectares, hosts large, small, and medium-sized industrial and production service activities and an urban service center. In addition,

the Santa Gilla lagoon region is home to Tiscali's technological research campus and production activities characterized by different levels of use (aquaculture activities, salt pans, agricultural activities, manufacturing activities, tourism activities). Furthermore, the new infrastructural developments financed by PNRR funds dedicated to Special Economic Zones support the enhancement of Cagliari's Canal Port.

### 2.5. Barrier Breaching Events

Breaching is likely to become more common as a result of sea-level rise and barrier island flooding [63]. The storm hit the Southern Sardinia coast in October 2018 and resulted in widespread overwashing and numerous breaches. Figure 5 shows the main breaching at La Playa on 10 October, which generated the collapse of the National Road SS195. It is to be noticed that SS195 is the emergency road to evacuate the population of Western Cagliari Municipality [29].



**Figure 5.** Barrier breaching at La Playa beach and collapse of SS 195 during the compound sea and lagoon flood of 10 October 2018.

Previous models generated from breaches of sand dikes focus on the expansion of the dune gap and find that breaches originate from head cutting and erosion of the barrier on the lagoon side of the gap [64,65]. Ref. [66] found that surge-level differences between ocean and bay, and the resulting water level gradients, regulate flow conditions and are an important predictor of barrier island breaching. Site-specific process-based models of overwashing flows include XBeach [67], but the accuracy of the barrier breach prediction is still questionable [68].

Observations and modeling results of the event of October 2018 suggest that there is a particular emerging concern about compound water-level extremes, when conditions are extreme in more than one water body. Ref. [69] proposed a conceptual model postulating that the “breach susceptibility” [70] of a barrier beach is mainly related to the sea-back-barrier water level gradient. Water levels may become elevated in the back barrier with respect to the sea as the result of a wide range of processes [71], being runoff from upland precipitation is the main force at S.Gilla lagoon. Figure 6 shows the conceptual model adopted for predicting the morphologic impact of storms under sea-level variation on the La Playa barrier beach. In the examined extreme compound events, the hydraulic gradient was proven to drive a flow from the basin to the seaside as reported by [72]. This flow can potentially lead to sediment deposition on the seaward side of a barrier island.

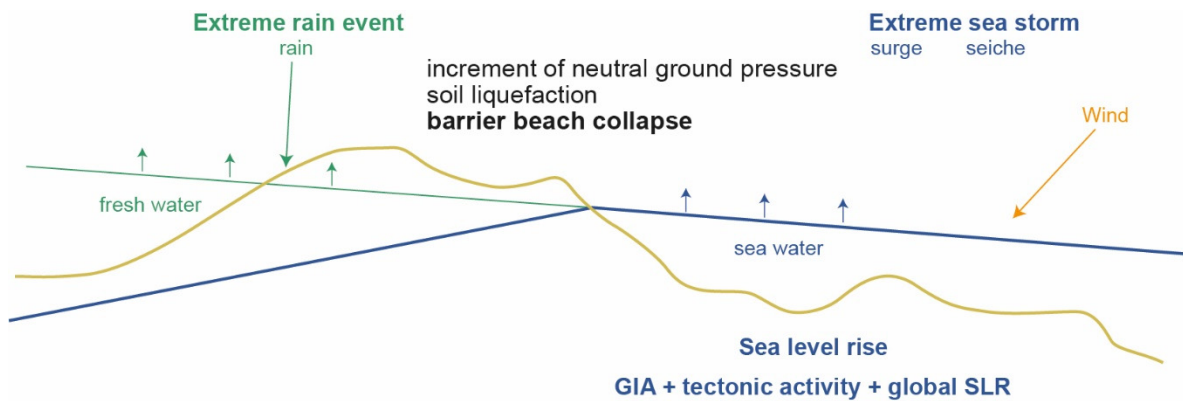


**Figure 6.** Conceptual model of barrier beach breaching.

The model of the breach-induced flood at La Playa is composed of two uncoupled modeling phases. The conceptual model of barrier breaching is used to calculate the occurrence of a wide breach development that significantly increases the exposure of the landward side of the S.Gilla lagoon to the combined effect of trends in  $H_s$  and sea level.

### 3. Results

Here, linear temporal trends are estimated using univariate linear regression models assuming low temporal correlation and Gaussian-distributed errors. The regression slope coefficient is assumed as the trend. Different datasets were considered. Specifically to the wave dataset, analysis of the annual maximum wave heights shows a positive trend over the last decades along the ordinary least square equation ( $R^2 = 0.92$ ) ( $H_{(s,max)} = 0.008 t - 12.245$  being the rate equal to  $+8 \text{ mm yr}^{-1}$  (Figure 7). Increases in mean annual heights have been slightly smaller than the maximum condition, the former with a rate equal to  $+5 \text{ mm yr}^{-1}$  (Figure 8). As expected, the seasonal trend shows a strong positive trend in the winter dataset of both mean and maximum, while mean and maximum wave heights have been decreasing during the summer. Also, we found that all trends have  $p$  values between 0.01 and 0.045, less than the predetermined significance level of 0.05.

Global mean sea level will continue to rise during the 21st century. Under all RCP scenarios, the rate of sea level rise will very likely exceed the observed rate of  $2.0 [1.7\text{--}2.3] \text{ mm yr}^{-1}$  during 1971–2010, with the rate of rise for RCP8.5 during 2081–2100 of 8 to  $16 \text{ mm yr}^{-1}$  (medium confidence). Based on the 1999–2021 high-accuracy sea-level dataset at the Cagliari station of the National Tidegauge Network (Rete Mareografica Nazionale—RMN), we estimate a rate of rise in the Gulf of Cagliari of  $5.4 \text{ mm yr}^{-1}$  (Figure 9).

Extreme wave analysis (EWA) of the ESA–CCI wave dataset was performed with a Gumbel distribution using the method of moments to estimate the best-fitting distribution. A 2-year return time event was selected as representative of frequent, low-magnitude events that could affect the system vulnerability at different spatial scales. The propagation of the offshore wave data from the mouth of the Gulf of Cagliari to the nearshore area has been simulated with the MIKE 21 Spectral Wave (SW) model, one of the state-of-the-art numerical modeling tools for studying spectral wind-wave modeling [73]. The conditions obtained at the extraction point of that field corresponding to the wave-breaking area were used in the Stockdon empirical wave run-up model. Figure 10 shows the flooded area in two selected scenarios, namely, in 2050 and 2010. At the territorial scale, the comparison of the two flooded areas shows a moderate increase equal to 23% when the time horizon grows (Figure 10). At the local scale, moving from 2050 to 2100 in the La Playa barrier beach shows how the entire beach will be flooded including a major part of the SS195 (Figure 11).

This flood ordinary scenario foresees a flattening of the submerged morphologies leading to a morphological simplification, dismantling the geomorphological characteristics of the lagoon-estuary and triggering the process of marine embayment.

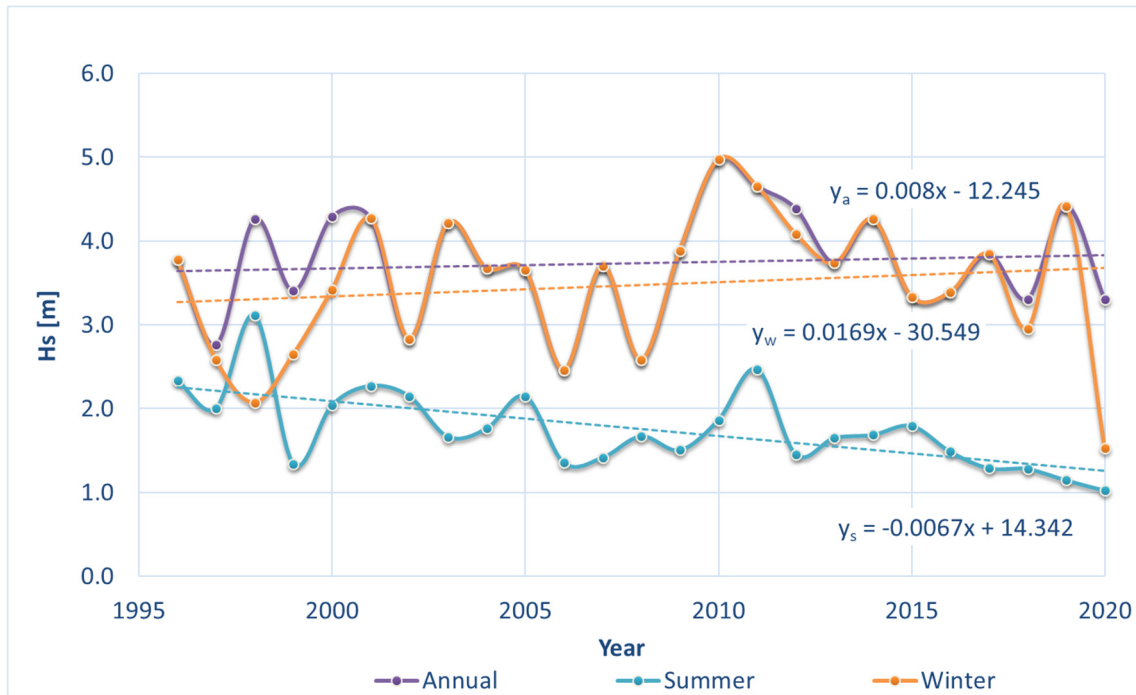


Figure 7. Trend analysis of annual and seasonal maximum wave heights.

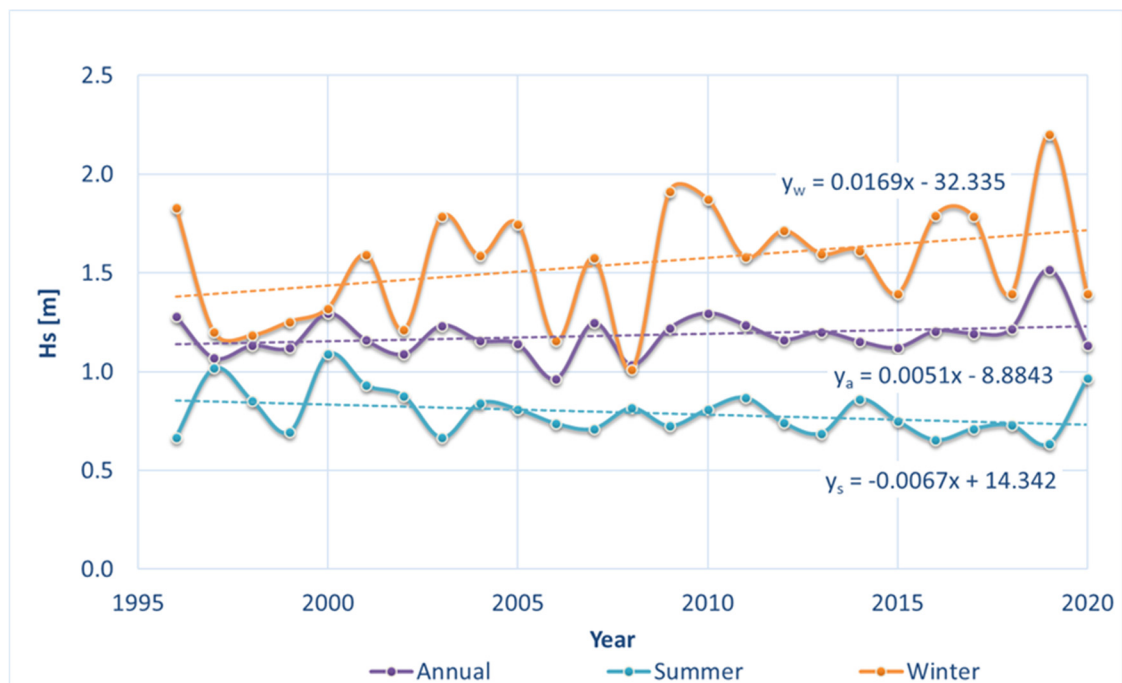


Figure 8. Trend analysis of annual and seasonal mean wave heights.

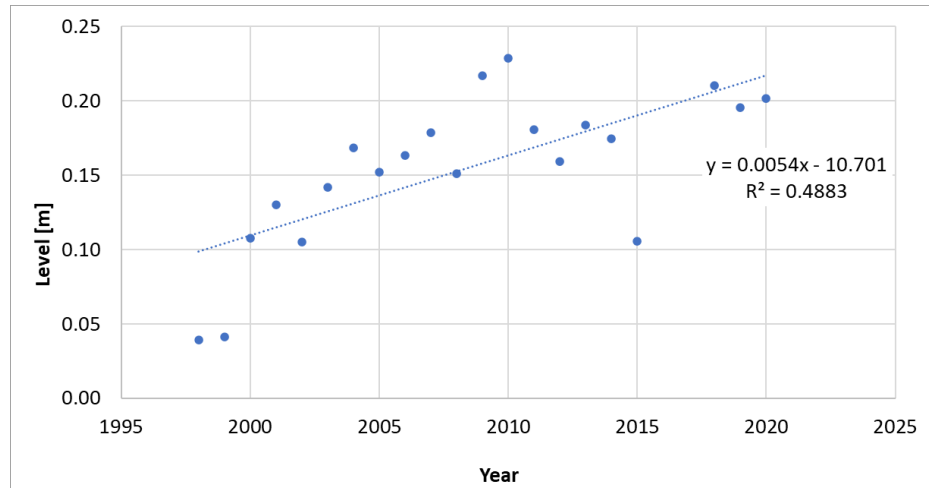


Figure 9. Trend analysis of annual mean sea level in Cagliari RMN station.

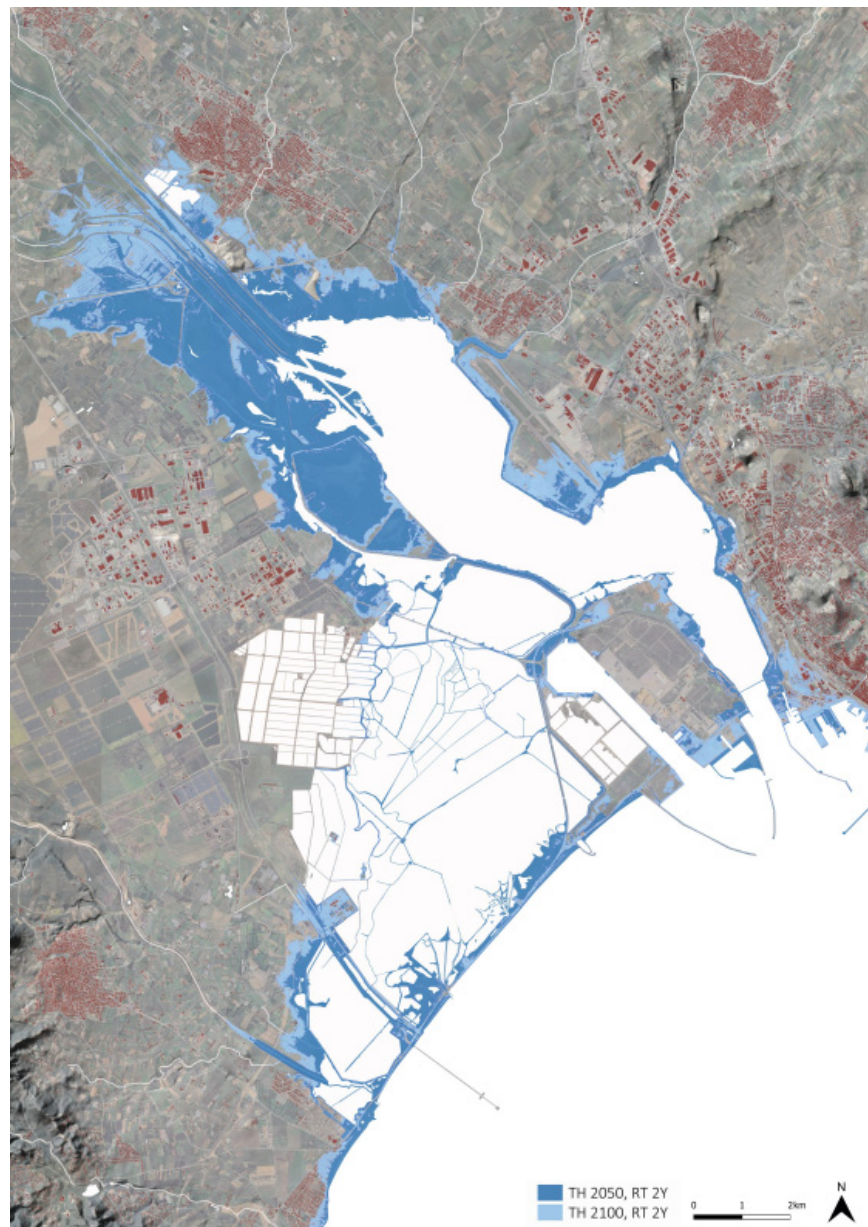
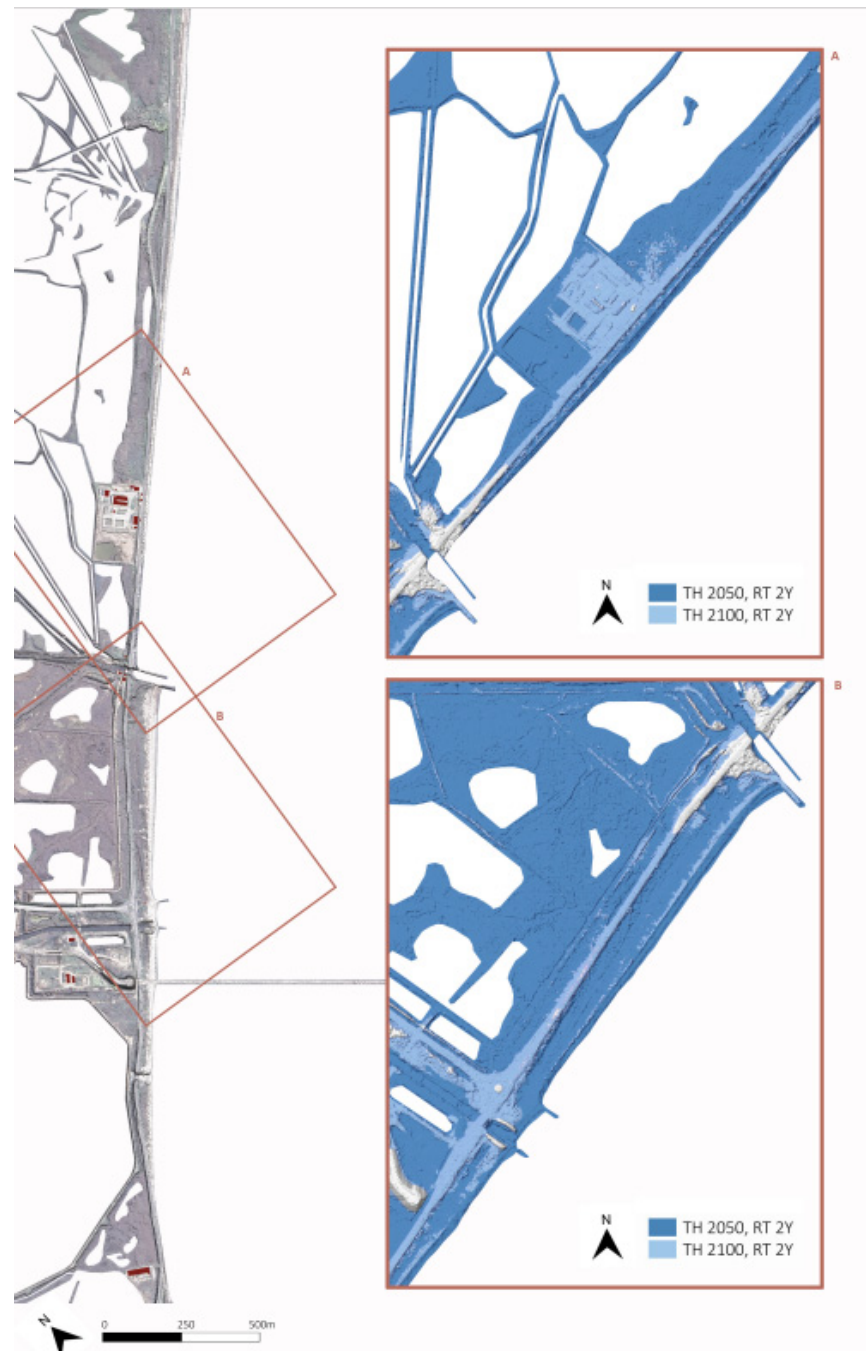


Figure 10. Sea coastal flooding in the 2050 and 2100 scenarios for a 2-year return time event: territorial scale.



**Figure 11.** Flooded areas in 2050 and 2100. Local scale on the La Playa barrier beach.

#### 4. Discussion

In conditions of complete naturalness of the regime of tributaries of water, with a considerable amount of sediments introduced into the system sufficient to compensate for the morphological response due to SLR, the systems of a natural barrier island could counteract the submersion through a morphological change of elevation (roll-over) or be overtaken by rapid submersion, as occurred during the Holocene in the northern Adriatic, but also in the Gulf of Oristano.

On the contrary, the urban lagoon barrier system of La Playa is stiffened by maritime works surmounted by roads with artificially channeled river mouths and solid transport slowed down by works along the riverbeds. There is, therefore, an opposite reaction to SLR, due to the lack of morphological degree of freedom. Modeling results show the

morphological response of the barrier beach at La Playa. The possible beach adaptation response will create a littoral system in disequilibrium with sediment-starved coastal strands. Based on local temporal trends in  $H_s$  ( $8 \text{ mm yr}^{-1}$ ) and sea level (SLR of  $5.4 \text{ mm yr}^{-1}$ ), new adaptation strategies should be adopted in the design of coastal protection to reduce that disequilibrium trend.

In a wider perspective, the analysis of the above model results is used to produce “questions of interest” [74] rather than “exact” predictions of the fundamental changes that will occur in the future. Here, the aim is to produce knowledge experiences/courses, which could support spatial planning activities for this environmental area. Model results, both numerical and analytical, highlight the main trends and indications of change in the environment structure. For this reason, models help to strengthen “exploratory scenarios”, i.e., scenarios that “describe, on the basis of a current situation and dominant trends, a series of events that necessarily lead to a possible future” [75]. Exploratory scenarios, being knowledge tools that envisage future environments, enable informed decision-making and prompt a capacity for future action. In this “scenario planning method” (SPM, [76]), the used models and techniques have a dual nature: a descriptive dimension that explores the environmental context of the lagoon in its internal dynamics and an instrumental dimension that questions the long-term static and dynamic impacts; the former being linked to the global level studies of the IPCC and to the specificities of the Mediterranean area and the latter showing the static impacts of sea-level changes and dynamic impacts at a local level.

The SPM allows us to explore under which conditions and where the vulnerabilities of the coastal system become more significant. The 2050 scenario is used as a projected scenario in line with the current state of the lagoon. The continuity refers to the design approaches: Additional sea and lagoon defense works will be required to protect the urban banks of the lagoon and the coastal strip infrastructures. To offset the system’s vulnerability in this scenario, further reinforcement of the banks is needed: this makes the current configuration and urban structure stable.

This artificial reinforcement/stiffening generates local vulnerability, because of the interference between the perspectives outlined in the models and the current municipal plans for special areas (port, airport, industrial areas), for transport and infrastructure plans.

The system is also vulnerable locally as a result of the “coastal squeeze”. It describes the process in which sea-level rise and other factors and sea storms push coastal habitats toward land. Coastal defenses create a static, artificial margin that squeezes the habitats of the system into a restricted area due to the erosion process [77]. The adaptation process to SLR, or extreme weather and climate events, is thus obstructed: The movement of habitats towards land to maintain their relative position to wave and tidal forces is effectively denied. In this system, the La Playa beach is a coastal space “squeezed” between the coastline and the coastal infrastructure [29]; then, the processes of natural adaptation of the Santa Gilla ecosystem to extreme events are limited by the pressure of urban infrastructure. This scenario enforces a constant approach to mitigation and emergency. Rigid structures within the area of direct wave influence, such as the existing coastal road 195, accentuate local vulnerability to coastal erosion phenomena and produce vulnerabilities at a territorial scale. SS195 is a strategic infrastructural connection between the capital city, Cagliari, and the south-western coast of the island. Moreover, it attracts daily a multiplicity of people and goods movements. The absence of connectivity puts residents of a vast urban area at risk of losing access to critical services that are vital for city living (hospitals, transport infrastructures, extra-local urban services, and schools). It also exposes them to the loss of safe travel conditions in relation to the greater fragility of the coastal strip where the SS 195 is located.

In the 2100 scenario, the flattening of the submerged morphologies triggers the process of marine embayment. In fact, the spatial layout and system ecological balance will change. The scenario draws attention to an alternative image and new environmental representations of this urban region. Indeed, a new internal gulf will be created and the present settlements (built-up areas, industrial areas, service centers, etc.) close to the new shoreline will face new forcing and dynamics. This spatial representation imposes new visions for the future and different land use. It prompts a review of the planning hypotheses of the municipalities located on the banks of the lagoon and, at the same time, offers unprecedented possibilities for city regeneration processes. It also requires infrastructures to change in perspective for the new development. In the 2100 scenario, the spatial organization of the new inner gulf of the metropolitan system confines the Canal Port area into an island. It will be anchored to the mainland by road infrastructure. To reduce its local vulnerability and thus maintain the planned and currently planned facilities (service and research centers, new ro-ro terminal, nautical and shipbuilding hub), new coastal defense infrastructures will be necessary. The same problem will arise for the airport area or the industrial areas on the banks of the lagoon.

## 5. Conclusions

In this paper, the construction of compound future projections of static (relative sea level) and dynamic (wind-wave) impacts on the vulnerable sandy coastal plan at S.Gilla lagoon supports the construction of planning scenarios at two different time horizons (2050 and 2100). These scenarios can support decision-making processes that have very different visions of the future: Alternative strategies identify future urban planning actions in relation to the resulting spatial organization. Based on local temporal trends in  $H_s$  ( $8 \text{ mm yr}^{-1}$ ) and sea level ( $5.4 \text{ mm yr}^{-1}$ ), a 2-year return time flood scenario at 2100 was selected to identify the high level of vulnerability at the territorial scale. The simplified conceptual breaching model coupled with a numerical flood model shows that the flattening of the submerged morphologies triggers the process of marine embayment. This defines a new waterfront in the landward part of S.Gilla lagoon, where new effective coastal adaptation strategies are needed. The results of these formal models can support new paradigms of design able to deal with relevant complexity and uncertainty.

**Author Contributions:** Conceptualization, A.S., A.A., F.A., P.E.O. and S.S.; methodology, A.S., A.A., F.A. and P.E.O.; validation, A.S., A.C., G.D., F.A. and V.L.P.; formal analysis, A.S., A.C., F.A. and P.E.O.; investigation, A.S., F.A., P.E.O. and V.L.P.; data curation, A.S., A.C., G.D., F.A. and V.L.P.; writing—original draft preparation, A.S., P.E.O. and S.S.; writing—review and editing, A.S. and A.C. All authors have read and agreed to the published version of the manuscript.

**Funding:** This research received no external funding.

**Institutional Review Board Statement:** Not applicable.

**Informed Consent Statement:** Not applicable.

**Data Availability Statement:** The raw data supporting the conclusions of this article will be made available by the authors on request.

**Conflicts of Interest:** The authors declare no conflict of interest.

## References

1. Frederikse, T.; Landerer, F.W.; Caron, L.; Adhikari, S.; Parkes, D.; Humphrey, V.; Dangendorf, S.; Hogarth, P.; Zanna, L.; Cheng, L.; et al. The causes of sea-level rise since 1900. *Nature* **2020**, *584*, 393–397. [[CrossRef](#)] [[PubMed](#)]
2. Marcos, M.; Tsimplis, M.N. Comparison of results of AOGCMs in the Mediterranean Sea during the 21st century. *J. Geophys. Res. Oceans* **2008**, *113*. [[CrossRef](#)]



3. Orlić, M.; Pasarić, M.; Pasarić, Z. Mediterranean Sea-Level Variability in the Second Half of the Twentieth Century: A Bayesian Approach to Closing the Budget. *Pure Appl. Geophys.* **2018**, *175*, 3973–3988. [[CrossRef](#)]
4. Calafat, F.M.; Wahl, T.; Tadesse, M.G.; Sparrow, S.N. Trends in Europe storm surge extremes match the rate of sea-level rise. *Nature* **2022**, *603*, 841–845. [[CrossRef](#)]
5. Nicholls, R.J.; Cazenave, A. Sea-Level Rise and Its Impact on Coastal Zones. *Science* **2010**, *328*, 1517–1520. [[CrossRef](#)] [[PubMed](#)]
6. Brichenno, L.M.; Wolf, J. Future wave conditions of Europe, in response to high-end climate change scenarios. *J. Geophys. Res. Oceans* **2018**, *123*, 8762–8791. [[CrossRef](#)]
7. Meucci, A.; Young, I.R.; Hemer, M.; Kirezci, E.; Ranasinghe, R. Projected 21st century changes in extreme wind-wave events. *Sci. Adv.* **2020**, *6*, eaaz7295. [[CrossRef](#)] [[PubMed](#)]
8. Timmermans, B.W.; Gommenginger, C.P.; Dodet, G.; Bidlot, J. Global Wave Height Trends and Variability from New Multimission Satellite Altimeter Products, Reanalyses, and Wave Buoys. *Geophys. Res. Lett.* **2020**, *47*, e2019GL086880. [[CrossRef](#)]
9. Morim, J.; Vitousek, S.; Hemer, M.; Reguero, B.; Erikson, L.; Casas-Prat, M.; Wang, X.L.; Semedo, A.; Mori, N.; Shimura, T.; et al. Global-scale changes to extreme ocean wave events due to anthropogenic warming. *Environ. Res. Lett.* **2021**, *16*, 074056. [[CrossRef](#)]
10. Ribal, A.; Young, I.R. 33 years of globally calibrated wave height and wind speed data based on altimeter observations. *Sci. Data* **2019**, *6*, 77. [[CrossRef](#)]
11. Sen, P.K. Estimates of the regression coefficient based on Kendall's tau. *J. Am. Stat. Assoc.* **1968**, *63*, 1379–1389. [[CrossRef](#)]
12. Theil, H. A rank-invariant method of linear and polynomial regression analysis. In *Henri Theil's Contributions to Economics and Econometrics. Advanced Studies in Theoretical and Applied Econometrics*; Raj, B., Koerts, J., Eds.; Springer: Dordrecht, The Netherlands, 1992; Volume 23, pp. 345–381. [[CrossRef](#)]
13. Ghanavati, M.; Young, I.; Kirezci, E.; Ranasinghe, R.; Duong, T.M.; Luijendijk, A.P. An assessment of whether long-term global changes in waves and storm surges have impacted global coastlines. *Sci. Rep.* **2023**, *13*, 11549. [[CrossRef](#)] [[PubMed](#)]
14. Vanem, E.; Walker, S.-E. Identifying trends in the ocean wave climate by time series analyses of significant wave height data. *Ocean Eng.* **2013**, *61*, 148–160. [[CrossRef](#)]
15. Lionello, P.; Conte, D.; Marzo, L.; Scarascia, L. The contrasting effect of increasing mean sea level and decreasing storminess on the maximum water level during storms along the coast of the Mediterranean Sea in the mid 21st century. *Glob. Planet. Chang.* **2017**, *151*, 80–91. [[CrossRef](#)]
16. Bonaldo, D.; Buchignani, E.; Pomaro, A.; Ricchi, A.; Sclavo, M.; Carniel, S. Wind waves in the Adriatic Sea under a severe climate change scenario and implications for the coasts. *Int. J. Clim.* **2020**, *40*, 5389–5406. [[CrossRef](#)]
17. Reale, M.; Narvaez, W.D.C.; Cavicchia, L.; Conte, D.; Coppola, E.; Flaounas, E.; Giorgi, F.; Gualdi, S.; Hochman, A.; Li, L.; et al. Future projections of Mediterranean cyclone characteristics using the Med-CORDEX ensemble of coupled regional climate system models. *Clim. Dyn.* **2021**, *58*, 2501–2524. [[CrossRef](#)]
18. Ulbrich, U.; Leckebusch, G.C.; Pinto, J.G. Extra-tropical cyclones in the present and future climate: A review. *Theor. Appl. Clim.* **2009**, *96*, 117–131. [[CrossRef](#)]
19. Bengtsson, L.; Hodges, K.I. On the evaluation of temperature trends in the tropical troposphere. *Clim. Dyn.* **2009**, *36*, 419–430. [[CrossRef](#)]
20. Lionello, P.; Malanotte-Rizzoli, P.; Boscolo, R.; Alpert, P.; Artale, V.; Li, L.; Luterbacher, J.; May, W.; Trigo, R.; Tsimplis, M. The Mediterranean climate: An overview of the main characteristics and issues. *Dev. Earth Environ. Sci.* **2006**, *4*, 1–26. [[CrossRef](#)]
21. De Leo, F.; De Leo, A.; Besio, G.; Briganti, R. Detection and quantification of trends in time series of significant wave heights: An application in the Mediterranean Sea. *Ocean Eng.* **2020**, *202*, 107155. [[CrossRef](#)]
22. Mentaschi, L.; Besio, G.; Cassola, F.; Mazzino, A. Performance evaluation of Wavewatch III in the Mediterranean Sea. *Ocean Model.* **2015**, *90*, 82–94. [[CrossRef](#)]
23. Sierra, J.P.; Castrillo, R.; Mestres, M.; Mössö, C.; Lionello, P.; Marzo, L. Impact of Climate Change on Wave Energy Resource in the Mediterranean Coast of Morocco. *Energies* **2020**, *13*, 2993. [[CrossRef](#)]
24. Casas-Prat, M.; Sierra, J.P. Projected future wave climate in the NW Mediterranean Sea. *J. Geophys. Res. Oceans* **2013**, *118*, 3548–3568. [[CrossRef](#)]
25. Booij, N.; Ris, R.C.; Holthuijsen, L.H. A third-generation wave model for coastal regions: 1. Model description and validation. *J. Geophys. Res. Oceans* **1999**, *104*, 7649–7666. [[CrossRef](#)]
26. IPCC. 2007: Climate Change 2007: Synthesis Report. In *Contribution of Working Groups I, II and III to the Fourth Assessment Report of the Intergovernmental Panel on Climate Change*; Pachauri, R.K., Reisinger, A., Eds.; IPCC: Geneva, Switzerland, 2007; 104p.
27. Alves, J.H.G.M.; Young, I.R. On estimating extreme wave heights using combined Geosat, TOPEX/Poseidon and ERS-1 altimeter data. *Appl. Ocean Res.* **2003**, *25*, 167–186. [[CrossRef](#)]
28. Morim, J.; Hemer, M.; Wang, X.L.; Cartwright, N.; Trenham, C.; Semedo, A.; Young, I.; Brichenno, L.; Camus, P.; Casas-Prat, M.; et al. Robustness and uncertainties in global multivariate wind-wave climate projections. *Nat. Clim. Chang.* **2019**, *9*, 711–718. [[CrossRef](#)]

29. Sulis, A.; Serreli, S.; Carboni, A. A coupled approach for planning in vulnerable coastal landscapes. *Environ. Model. Softw.* **2023**, *172*, 105906. [\[CrossRef\]](#)
30. Fontolan, G.; Pillon, S.; Bezzi, A.; Villalta, R.; Lipizer, M.; Triches, A.; Daietti, A. Human impact and the historical transformation of saltmarshes in the Marano and Grado lagoon, northern Adriatic sea. *Estuar. Coast. Shelf Sci.* **2012**, *113*, 41–56. [\[CrossRef\]](#)
31. Antonioli, F.; Anzidei, M.; Amorosi, A.; Presti, V.L.; Mastronuzzi, G.; Deiana, G.; De Falco, G.; Fontana, A.; Fontolan, G.; Lisco, S.; et al. Sea-level rise and potential drowning of the Italian coastal plains: Flooding risk scenarios for 2100. *Quat. Sci. Rev.* **2017**, *158*, 29–43. [\[CrossRef\]](#)
32. Deiana, G.; Lecca, L.; Melis, R.T.; Demurtas, V.; Orrù, P.E. Submarine geomorphology of the southwestern sardinian continental shelf (Mediterranean sea): Insights into the last glacial maximum sea-level changes and related environments. *Water* **2021**, *13*, 155. [\[CrossRef\]](#)
33. Lecca, L. La piattaforma continentale miocenico-quadernaria del margine occidentale sardo: Blocco diagramma sezionato. *Rend. Sem. Fac. Sci. Univ. Cagliari.* **2000**, *1*, 49–70.
34. Orrù, P.E.; Demurtas, V.; Meleddu, A.; Paliaga, E.; Todde, S.; Deiana, G. Geohazard features of the Southern Sardinia. *J. Maps* **2024**, *20*, 2375093. [\[CrossRef\]](#)
35. De Muro, S.; Orrù, P. Il contributo delle beachrock nello studio della risalita del mare olocenico. Le beachrock post-glaciali della Sardegna nord orientale. *J. Quat. Sci.* **1998**, *11*, 19–39.
36. Orrù, P.E.; Antonioli, F.; Lambeck, K.; Verrubbi, V. *Holocene Sea-Level Change in the Cagliari Coastal Plain*; Quaternaria Nova, VIII: South Sardinia, Italy, 2004; pp. 193–210.
37. De Falco, G.; Antonioli, F.; Fontolan, G.; Lo Presti, V.; Simeone, S.; Tonielli, R. Early cementation and accommodation space dictate the evolution of an overstepping barrier system during the Holocene. *Mar. Geol.* **2015**, *369*, 52–56. [\[CrossRef\]](#)
38. Solinas, E.; Orrù, P. Santa Gilla: Spiagge sommerse e frequentazione di epoca punica. In *Aequora, Pontos, Jam, Mare... Mare, Uomini e Mercè nel Mediterraneo Antico. Atti del Convegno Internazionale (Genova, 9–10 Dicembre 2004)*; Giannattasio, B.M., Ed.; All'Insegna del Giglio: Firenze, Italy, 2006; pp. 249–252.
39. Antonioli, F.; Anzidei, M.; Lambeck, K.; Auriemma, R.; Gaddi, D.; Furlani, S.; Orrù, P.E.; Solinas, E.; Gaspari, A.; Karinja, S.; et al. Sea level change during the Holocene in Sardinia and in the North-eastern Adriatic (Central Mediterranean sea) from archaeological and geomorphological data. *Quat. Sci. Rev.* **2007**, *26*, 2463e2486. [\[CrossRef\]](#)
40. Buosi, C.; Del Rio, M.; Orrù, P.; Pittau, P.; Scanu, G.G.; Solinas, E. Sea level changes and past vegetation in the Punic period (5th–4th century BC): Archaeological, geomorphological and palaeobotanical indicators (South Sardinia—West Mediterranean Sea). *Quat. Int.* **2017**, *439*, 141–157. [\[CrossRef\]](#)
41. Orrù, P.E.; Solinas, E.; Puliga, G.; Deiana, G. Palaeo-shorelines of the history period, sant' Antioco Island, south-western Sardinia (Italy). *Quat. Int.* **2011**, *232*, 71e81. [\[CrossRef\]](#)
42. Antonioli, F.; Presti, V.L.; Rovere, A.; Ferranti, L.; Anzidei, M.; Furlani, S.; Mastronuzzi, G.; Orrù, P.E.; Scicchitano, G.; Sannino, G.; et al. Reply to comment by Evelpidu N., and Pirazzoli P. on “Tidal notches in the Mediterranean sea: A comprehensive analysis”. *Quat. Sci. Rev.* **2016**, *131*, 238–241. [\[CrossRef\]](#)
43. El-Sayed, M.K. Beachrock cementation in Alexandria, Egypt. *Mar. Geol.* **1988**, *80*, 29–35. [\[CrossRef\]](#)
44. Mastronuzzi, G.; Palmentola, G.; Sansò, P. Some Theoretic aspects of rocky coast dynamics. *Boll. Oceanol. Teor. Appl.* **1992**, *10*, 109–115.
45. Devoti, R.; D'Agostino, N.; Serpelloni, E.; Pietrantonio, G.; Riguzzi, F.; Avallone, A.; Cavaliere, A.; Cheloni, D.; Cecere, G.; D'Ambrosio, C.; et al. A Combined Velocity Field of the Mediterranean Region. *Ann. Geophys.* **2017**, *60*, 0215. [\[CrossRef\]](#)
46. Aucelli, P.P.C.; Di Paola, G.; Incontri, P.; Rizzo, A.; Vilardo, G.; Benassai, G.; Buonocore, B.; Pappone, G. Coastal Inundation Risk Assessment Due to Subsidence and Sea Level Rise in a Mediterranean Alluvial Plain (Volturno Coastal Plain—Southern Italy). *Estuar. Coast. Shelf Sci.* **2017**, *198*, 597–609. [\[CrossRef\]](#)
47. Lambeck, K.; Antonioli, F.; Anzidei, M.; Ferranti, L.; Leoni, G.; Scicchitano, G.; Silenzi, S. Sea level change along the Italian coast during the Holocene and projections for the future. *Quat. Int.* **2011**, *232*, 250–257. [\[CrossRef\]](#)
48. Orrù, P.E.; Mastronuzzi, G.; Deiana, G.; Pignatelli, C.; Piscitelli, A.; Solinas, E.; Spanu, P.G.; Zucca, R. Sea level changes and geoarchaeology between the bay of Capo Malfatano and Piscinnì Bay (SW Sardinia) in the last 4 kys. *Quat. Int.* **2014**, *336*, 180–189. [\[CrossRef\]](#)
49. Ferranti, L.; Antonioli, F.; Amorosi, A.; Dai Prà, G.; Mastronuzzi, G.; Mauz, B.; Monaco, C.; Orrù, P.; Pappalardo, M.; Radtke, U.; et al. Elevation of the last interglacial highstand in Italy: A benchmark of coastal tectonics. *Quat. Int.* **2006**, *145*, 3–18.
50. Faccenna, C.; Speranza, F.; D'Ajello Caracciolo, F.; Mattei, M.; Oggiano, G. Extensional tectonics on Sardinia (Italy): In-sights into the arc-back-arc transitional regime. *Tectonophysics* **2002**, *356*, 213–232. [\[CrossRef\]](#)
51. Church, J.A.; Clark, P.U.; Cazenave, A.; Gregory, J.M.; Jevrejeva, S.; Levermann, A.; Merrifield, M.A.; Milne, G.A.; Nerem, R.S.; Nunn, P.D.; et al. Sea-Level Rise by 2100. *Science* **2013**, *342*, 1445. [\[CrossRef\]](#)

52. Rahmstorf, S. A Semi-Empirical Approach to Projecting Future Sea-Level Rise. *Science* **2007**, *315*, 368–370. [CrossRef] [PubMed]
53. Marsico, A.; Lisco, S.; Presti, V.L.; Antonioli, F.; Amorosi, A.; Anzidei, M.; Deiana, G.; De Falco, G.; Fontana, A.; Fontolan, G.; et al. Flooding scenario for four Italian coastal plains using three relative sea level rise models. *J. Maps* **2017**, *13*, 961–967. [CrossRef]
54. Rovere, A.; Raymo, M.E.; Vacchi, M.; Lorscheid, T.; Stocchi, P.; Gómez-Pujol, L.; Harris, D.L.; Casella, E.; O’Leary, M.J.; Hearty, P.J. The analysis of Last Interglacial (MIS 5e) relative sea-level indicators: Reconstructing sea-level in a warmer world. *Earth-Sci. Rev.* **2016**, *159*, 404–427. [CrossRef]
55. Stocchi, P.; Spada, G. Glacio and hydro-isostasy in the Mediterranean Sea: Clark’s zones and role of remote ice sheets. *Ann. Geophys.* **2009**, *50*. [CrossRef]
56. Landais, A.; Chappellaz, J.; Delmotte, M.; Jouzel, J.; Blunier, T.; Bourg, C.; Caillon, C.; Cherrier, S.; Malaize’, B.; Masson-Delmotte, V.; et al. A tentative reconstruction of the last interglacial and glacial inception in Greenland based on new gas measurements in the Greenland Ice Core Project (GRIP) ice core. *J. Geophys. Res.* **2003**, *108*, D18. [CrossRef]
57. Kawamura, K.; Nakazawa, T.; Aoki, S.; Sugawara, S.; Fujii, Y.; Watanabe, O. Atmospheric CO<sub>2</sub> variations over the last three glacial-interglacial climatic cycles deduced from the Dome Fuji deep ice core, Antarctica using a wet extraction technique. *Tellus B Chem. Phys. Meteorol.* **2003**, *55*, 126–137. [CrossRef]
58. Ardhuin, F.; Stopa, J.E.; Chapron, B.; Collard, F.; Husson, R.; Jensen, R.E.; Johannessen, J.; Mouche, A.; Passaro, M.; Quartly, G.D.; et al. Observing Sea States. *Front. Mar. Sci.* **2019**, *6*, 124. [CrossRef]
59. Queffeuilou, P. Long-Term Validation of Wave Height Measurements from Altimeters. *Mar. Geodesy* **2004**, *27*, 495–510. [CrossRef]
60. Dodet, G.; Piolle, J.-F.; Quilfen, Y.; Abdalla, S.; Accensi, M.; Ardhuin, F.; Ash, E.; Bidlot, J.-R.; Gommenginger, C.; Marechal, G.; et al. The Sea State CCI dataset v1: Towards a sea state climate data record based on satellite observations. *Earth Syst. Sci. Data* **2020**, *12*, 1929–1951. [CrossRef]
61. Piollé, J.-F.; Dodet, G.; Ash, E. ESA Sea State Climate Change Initiative: Product User Guide, Version 1.0. 2020. Available online: [http://dap.ceda.ac.uk/thredds/fileServer/neodc/esacci/sea\\_state/docs/v1.1/Sea\\_State\\_cci\\_PUG\\_v1.0-signed.pdf](http://dap.ceda.ac.uk/thredds/fileServer/neodc/esacci/sea_state/docs/v1.1/Sea_State_cci_PUG_v1.0-signed.pdf) (accessed on 10 November 2024).
62. Soro, L. Testimonianze materiali per una conoscenza dell’area interessata dalla cittadella di Sancta Ygia dal passaggio tra la dominazione dei bizantini allo stanziamento dei Giudici. In *Città tra Mare e Laguna: Da Santa Gilla a Cagliari*; Martorelli, R., Serreli, G., Mele, M.G.R., Nocco, S., Eds.; UNICApres/Ateneo: Cagliari, Italy, 2023.
63. Passeri, D.L.; Dalyander, P.S.; Long, J.W.; Mickey, R.C.; Jenkins, R.L.; Thompson, D.M.; Plant, N.G.; Godsey, E.S.; Gonzalez, V.M. The Roles of Storminess and Sea Level Rise in Decadal Barrier Island Evolution. *Geophys. Res. Lett.* **2020**, *47*, e2020GL089370. [CrossRef]
64. Visser, P.J. A model for breach erosion in sand-dikes. In *Proceedings of the Coastal Engineering Conference*; Edge, B.L., Ed.; American Society of Civil Engineers (ASCE): Reston, VA, USA, 2001; Volume 4, pp. 3829–3842.
65. Tuan, T.Q.; Stive, M.J.; Verhagen, H.J.; Visser, P.J. Process-based modeling of the overflow-induced growth of erosional channels. *Coast. Eng.* **2008**, *55*, 468–483. [CrossRef]
66. Basco, D.R.; Shin, C.S. A one-dimensional numerical model for storm-breaching of barrier islands. *J. Coast. Res.* **1999**, *15*, 241–260.
67. Roelvink, D.; Reniers, A.; Van Dongeren, A.; van Thiel De Vries, J.; McCall, R.; Lescinski, J. Modelling storm impacts on beaches, dunes and barrier islands. *Coast. Eng.* **2009**, *56*, 1133–1152. [CrossRef]
68. Nienhuis, J.H.; van de Wal, R.S.W. Projections of Global Delta Land Loss From Sea-Level Rise in the 21st Century. *Geophys. Res. Lett.* **2021**, *48*, e2021GL093368. [CrossRef]
69. Engelstad, A.; Ruessink, B.; Wesselman, D.; Hoekstra, P.; Oost, A.; van der Vegt, M. Observations of waves and currents during barrier island inundation. *J. Geophys. Res. Oceans* **2017**, *122*, 3152–3169. [CrossRef]
70. Kraus, C.; Militello, A.; Todoroff, G. Barrier breaching processes and barrier spit breach, stone lagoon, California. *Shore Beach* **2002**, *70*, 21–28.
71. Goff, J.A.; Swartz, J.M.; Gulick, S.P.; Dawson, C.N.; de Alegria-Arzaburu, A.R. An outflow event on the left side of Hurricane Harvey: Erosion of barrier sand and seaward transport through Aransas Pass, Texas. *Geomorphology* **2019**, *334*, 44–57. [CrossRef]
72. Sherwood, C.R.; Long, J.W.; Dickhudt, P.J.; Dalyander, P.S.; Thompson, D.M.; Plant, N.G. Inundation of a barrier island (Chandeleur Islands, Louisiana, USA) during a hurricane: Observed water-level gradients and modeled seaward sand transport. *J. Geophys. Res. Earth Surf.* **2014**, *119*, 1498–1515. [CrossRef]
73. Sulis, S. Asproni, Modelling storm-induced beach evolution at La Playa beach, Sardinia, IT. In *Proceedings of the SCACR2015*, Florence, Italy, 28 September–1 October 2015.
74. Derbyshire, J.; Wright, G. Augmenting the intuitive logics scenario planning method for a more comprehensive analysis of causation. *Int. J. Forecast.* **2017**, *33*, 254–266. [CrossRef]
75. Julien, P.A.; Lamonde, P.; Latouche, D. La méthode des scénarios en prospective. *L’Actualité Économique* **1975**, *1*, 253–281. [CrossRef]

- 
76. Godet, M.; Durance, P. *La Prospectiva Estratégica. Para las Empresas y los Territorios*; Dunod Unesco: Paris, France, 2011.
  77. Doody, J.P. Coastal squeeze and managed realignment in southeast England, does it tell us anything about the future? *Ocean Coast. Manag.* **2013**, *79*, 34–41. [[CrossRef](#)]

**Disclaimer/Publisher’s Note:** The statements, opinions and data contained in all publications are solely those of the individual author(s) and contributor(s) and not of MDPI and/or the editor(s). MDPI and/or the editor(s) disclaim responsibility for any injury to people or property resulting from any ideas, methods, instructions or products referred to in the content.